International Biodeterioration & Biodegradation 206 (2026) 106215

Contents lists available at ScienceDirect

International Biodeterioration & Biodegradation

journal homepage: www.elsevier.com/locate/ibiod

Superficial rock decalcification by the lichen *Tephromela atra* var. *calcicola*: what's true?

Mauro Tretiach [a,*], Sofia Ceseri [a], Ornella Salvadori [b], Francesco Princivalle [c], Barbara Salvadori [d]

[a] Department of Life Sciences, University of Trieste, Via Giorgieri 10, 34127, Trieste, Italy
[b] Via Naviglio 19/A, 30032, Fiesso d'Artico, Italy
[c] Department of Mathematics, Informatics and Geosciences, Via Weiss 8, 34128, Trieste, Italy
[d] Institute of Heritage Science, National Research Council (ISPC-CNR), Via Madonna del Piano 10, Sesto Fiorentino, 50019, Italy

ARTICLE INFO

Keywords:
Biodeterioration
Calcite
Carbonate-rich substrate
Oxalates
FTIR
XRD

ABSTRACT

The thallus–substrate relationship of *Tephromela atra* var. *calcarea* was investigated to determine whether the colonisation of carbonate-rich rock can be related to a "superficial decalcification" of the substrate, as claimed by some authors. Fragments of thalli still adhering to the substrate from the TSB herbarium were embedded in epoxy resin to obtain cross-sections, which were analysed by FPA-FTIR microspectroscopy in reflection mode to acquire chemical imaging data reflecting the spatial distribution of molecular components. The cross-sections were then stained with periodic acid-Schiff, and the percentage of hyphal spread was measured in selected areas of 2 mm^2 at fixed distances along vertical transects from the thallus–substrate interface to the hyphal-free substrate. X-ray diffraction (XRD) was performed on additional fragments to detect any biomineralization products present. The hyphae of *T. atra* penetrated all calcareous substrates to a maximum depth of 0.8 mm, also piercing single calcite clasts. Hyphal spread varied greatly between substrates, with a minimum in compact limestone and a maximum in porous limestone. XRD analyses showed the presence of the biominerals whewellite and weddellite in varying amounts, and confirmed the presence of calcite in all samples, except in one occurring on Roman brick. High-resolution FTIR chemical maps showed the presence of calcite in medium/high to high concentration at the thallus–substrate interface. No evidence of calcite depletion was observed. These results do not support a significant carbonate depletion of the surface of the carbonate-rich rock colonised by *T. atra*, whose hyphae can actively penetrate the calcite clasts.

1. Introduction

Among the diverse organisms that colonise lithic substrates, lichens can be particularly damaging to the integrity of the rock, as the hyphae of the mycobiont can physically penetrate between the crystals, while various groups of organic substances can attack the mineral components, and eventually form biominerals which accumulate in the thallus and at the thallus–substrate interface (Gadd, 2021). Identifying the biomineralization products of lichens is a crucial step towards understanding thallus–substrate interactions and clarifying their effects on stone surface (Silva et al., 1999). In order to gain a deeper insight into these mechanisms, numerous analytical techniques have been used in the field of cultural heritage preservation in recent decades and are constantly being improved to achieve higher resolution and sensitivity. Pioneering work on the pedogenetic role of lichens has utilised techniques such as Differential Thermal Analysis (DTA) and Differential Thermogravimetric Analysis (DTG) (Mitchell et al. 1966; Syers et al. 1967; Ascaso and Galvan, 1976). These techniques were superseded by infrared (IR) spectroscopy, which was first introduced by Ascaso et al. (1982) to study the weathering of calcareous rocks. Nowadays, biomineralization products are frequently identified by X-ray Diffractometry (XRD), and Scanning Electron Microscopy coupled with Energy Dispersive Spectrometry (SEM-EDS). These methods contributed significantly to the study of *e.g.* the mechanisms of calcium oxalate deposit formation (Ascaso et al., 1982; Salvadori and Zitelli, 1981; Wilson et al. 1981), and the role of lichen compounds in the dissolution of minerals (Adamo and Violante, 2000). The main disadvantage of XRD is the relatively low sensitivity: Biomineralization products with

* Corresponding author. author
E-mail address: tretiach@units.it (M. Tretiach).

https://doi.org/10.1016/j.ibiod.2025.106215
Received 10 June 2025; Received in revised form 5 August 2025; Accepted 12 September 2025
Available online 17 September 2025

concentrations below c. 2 % are generally not detectable, and matrix effects must also be considered. This problem was bypassed by the introduction of Fourier transform (FT)-Raman spectroscopy, FT-infrared spectroscopy (FTIR) and by XRD instrumentation improvements. FT-Raman spectroscopy was first applied in a pioneering study on the effects of *Dirina massiliensis* f. *sorediata* on Renaissance frescoes (Edwards et al. 1991), and since then it has been applied to many other lichens (Prieto et al. 2000; Seaward et al. 1998; Edwards, 1997; Edwards et al. 1997, 2002, 2005). This technique allows to investigate the interface, the substratum, the incorporation of substratum material into the incrustation, as well as the lichen metabolites eventually present in the sample (Edwards et al. 1998, 1999; Edwards and Seaward, 1993; Holder et al. 2000; Seaward et al. 1995), with all the advantages of low laser power needed for the irradiation of the material. FTIR was first applied in a study on the bioalteration caused by lichens to the Greek monuments of Selinunte, Sicily (Gorgoni et al. 1992), with the advantage of a high resolution combined with the small amount of material requested for the analysis. Now it is certainly one of the most common methods adopted in the field of stone biodeterioration (*e.g.* Mazzotti et al. 2021; Pinna et al. 1998; Rampazzi, 2019; Scarciglia et al. 2012).

The last generation X-ray diffractometers improved accuracy, speed, and versatility for multiple applications without any manual intervention. X-ray microdiffraction was used for the first time in a study on the relationships between calcareous substrata and endolithic lichens (Pinna et al. 1998). Like FT-Raman spectroscopy, X-ray microdiffraction can be performed not only on powdered samples, but also directly on cross sections, with the great advantage that the analysis is performed on intact material, that can be used for subsequent analyses, such as specific staining or EDS microanalysis. It also provides information on the identity and distribution of the crystalline phases present (Appolonia et al. 1996). X-ray microdiffraction is now frequently used in the field of biodeterioration, as this technique is highly sensitive and non-destructive. These features are particularly important when sampling is a serious limitation, such as in the studies of art works.

In this study, high-resolution FPA FTIR-microspectroscopy is used, together with the last generation XRD, in a study on the thallus–substrate relationship of the lichen *Tephromela atra* var. *calcarea*. The aim is to verify the alleged "superficial decalcification" of the substratum that would explain the occasional presence of silicicolous lichens on carbonate-rich rock. This hypothesis was originally proposed by Asta and Roux (1977) in a paper on saxicolous lichen vegetation in the French Alps for rocks such as calcescist, flysch, gneiss and schist, which contain varying amounts of calcium carbonate and effervesce strongly to HCl 6 N at depth, but only slightly on the exposed surface. Further data in support of this phenomenon were presented by Asta and Lachet (1978), who explained the lower carbonate content in the superficial layer as a result of its progressive chemical dissolution by carbonic acid. In the following years, this explanation was extended by other authors to some lichens (among others: *Diploschistes actinostomous*, *Lecanora sulphurea*, *Lecidea fuscoatra, Lecidella asema*, *Placopyrenium bucekii*, *Rhizocarpum lecanorinum*, and *Tephromela atra s.lat.*; see Nimis and Tretiach, 1999), that typically grow on siliceous substrates and occasionally occur on calcareous rocks such as limestone and dolomite. This substrate shift (or rather expansion) is apparently more common in the perimediterranean regions, where it has been documented quite frequently (Nimis, 1993), and less so at higher latitudes (Wirth, 1995), although *T. atra* is known to occur on limestone, *e.g.*, in Öland, Sweden (Fröberg et al., 2006). If the "superficial decalcification" of calcescist, flysch, gneiss and schist is certainly a real fact (the chemical dissolution of the carbonates leaves a more porous substratum, enriched in the siliceous components), the same phenomenon seems unlikely in limestone and dolomite, composed of almost 100 % calcium carbonate ($CaCO_3$) or calcium/magnesium carbonate ($Ca/MgCO_3$).

The hypothesis of a "superficial decalcification" of limestone and dolomite was already refuted by Salvadori and Tretiach (2002) on the basis of XRD data of three lichens –- including *T. atra* – and their substrates but is nevertheless regularly taken up in the more recent literature (*e.g.* Bültmann, 2012; Bültmann et al., 2015; Nimis et al., 2018; Roux et al., 2025). We therefore considered it useful to provide additional data obtained through the most advanced techniques, which allowed for the spatial localization of molecular components (chemical imaging) with unprecedented precision, thus further refining previous interpretations.

2. Materials and methods

Ten specimens of *Tephromela atra* var. *calcarea* occurring on brick (n = 1), calcarenites (n = 6), calcareous schist (n = 1), and limestones (n = 2) were selected from the TSB herbarium, University of Trieste (Supplementary Information Table S1; species nomenclature according to Nimis, 2025). The samples were observed with a Leica MZ16 stereomicroscope and photomicrographs were taken with an iPhone 11 camera. Small fragments of the colonized substrates, measuring c. 10 × 15 × 10 mm or less, were sampled using a chisel and hammer.

2.1. Cross-sections: preparation, staining and characterization

A selection of the colonized substrate fragments was embedded in a two-component epoxy resin (2K, Borma Wachs B.P.S., Jesolo, IT), and polished using a manual polisher LS3V (Remet, IT) with P 50, 200, 600 and 1000 abrasive discs and then manually with P 1200 and 1500 abrasive paper under tap water. The cross-sections were photographed with a Wild Heerbrugg Leica M420 stereomicroscope and an iPhone 11 camera, and analysed by LUMOS II FTIR (see below). To investigate the penetration of the hyphae into the substrates, the cross-sections were stained with periodic acid-Schiff (PAS) according to Whitlatch and Johnson (1974), with minimal changes to the protocol (Supplementary Methods S1.1). The stained cross-sections were observed under the stereomicroscope, and a new series of stereophotographs was taken with a Canon EOS R10 camera and compared with the photomicrographs taken with the LUMOS II FTIR, to locate the exact spots where the FTIR analyses had been performed. The stereophotographs of each sample were used to measure thallus thickness using ImageJ software, while penetration of the hyphae into the substrate was quantified by graphical processing of the digital colour stereophotographs according to Ametrano et al. (2017), using software *Fiji* (ImageJ) and its *Color Segmentation* plugin (Supplementary Methods S1.2). To calculate the hyphal spread, i.e. the per cent area occupied by the hyphae in a cross section, a transect perpendicular to the outer surface was defined on each stained cross-section (Fig. 1), and a maximum of four to five rectangular areas of 2.5 mm × 0.8 mm (2 mm^2) were selected, starting from the outer surface, with each area 0.8 mm from the previous area.

2.2. Analysis of (bio-)minerals

To investigate the mineralogical composition of the substrate and any biomineralization products present, some of the fragments obtained from the herbarium specimens were ground in an agate mortar. Samples of 450–600 mg each were analysed with an Empyrean X-ray diffraction platform (Malvern Panalytical, UK) in Bragg-Brentano geometry, with Cu-Kα radiation source operating at 40 kV and 40 mA, automatic optics on both incident and diffracted beams and a strip detector working in 1D mode. Five scans for each sample were collected in the range 5–75 °2θ using a step interval of 0.0084 °2θ, with a step counting time of 15.24 s and then merged. To identify the mineral phases in each X-ray powder spectrum, the Panalytical Highscore Plus 3.0c software and PDF-2/ICSD databases were used.

To obtain information on the spatial distribution of the chemical compounds present at the thallus–substrate interface (chemical imaging), Fourier transform infrared (FTIR) spectroscopic analyses of polished, unstained cross-sections (see above) were performed using a LUMOS II FTIR microscope (Bruker Group, Bruker Optics, US) equipped

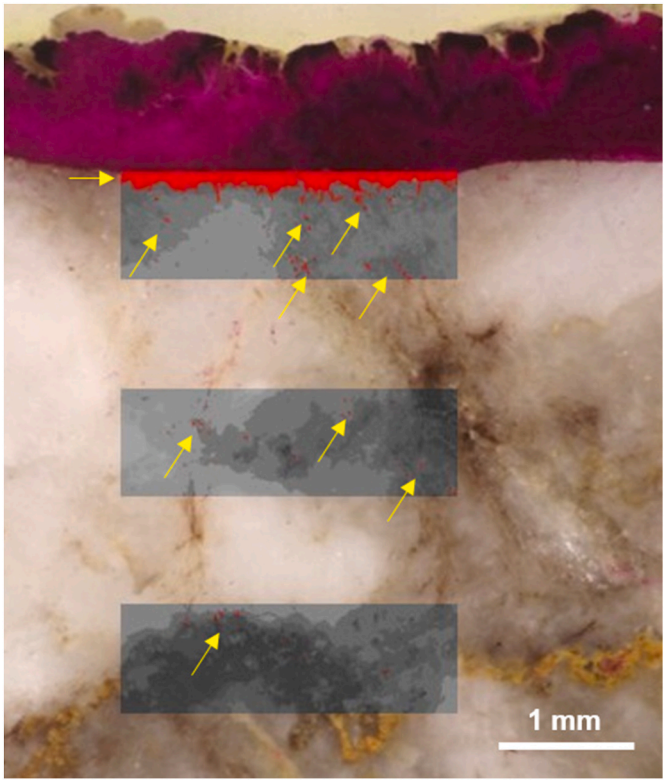

Fig. 1. Cross-section stereophotograph of *Tephomela atra* var. *calcarea* occurring on calcarenite (TSB 37937), stained with periodic acid-Schiff. The three grey areas arranged along a vertical transect were selected for the estimation of the percentage hyphal cover (PHC); the hyphae are highlighted in false colour (red) and eventually marked by yellow arrows. Further explanations in the main text. (For interpretation of the references to colour in this figure legend, the reader is referred to the Web version of this article.)

with a Focal Plane Array (FPA) detector (32 × 32 detector elements) cooled with liquid nitrogen. FPA-FTIR images (from one to three for each cross-section) were acquired in reflection mode within a spectral range of 4000–750 cm^{-1}, each as a single FTIR image (1024 spectra) covering a sampling area of approximately 150 × 150 μm^2, with a resolution of 4 cm^{-1} and co-adding 128 scans. Each individual spectrum in the FTIR image represents molecular information obtained from an area of approximately 5 × 5 μm^2 on the sample plane. The background was acquired, prior to measurements, on a gold mirror. The collected FTIR spectra were processed using OPUS 8.2 software.

2.3. Scanning electron microscopy (SEM) analysis

A selection of stained cross-sections (at least one per herbarium specimen) was mounted on aluminium stubs coated with double-sided carbon tape and then gold coated using the Emitech K550X sputter coater (Quorum Technologies, UK) with the pulsed rod evaporation method. Samples were analysed using a SEM Gemini 300 (Zeiss, DE); images were acquired by analysing secondary electrons, using an acceleration voltage of 5 kV and a working distance of 5 mm.

3. Results

The PAS-stained cross-sections (Figs. 1, 4–6) were used to morphometrically characterize the thalli of *T. atra* and their relationship to the substrate. Thallus thickness varied between samples, from a minimum of 0.40 mm (TSB 37462) to a maximum of 1.65 mm (TSB 38681) (Table 1). The hyphae of the medulla were directly associated with those that penetrated into the substrate, as could be observed by SEM in the samples that had been PAS-stained (Fig. 2a and b): the acidic solution caused a superficial dissolution of the carbonate, thus revealing a network of hyphae that were otherwise embedded in the rock matrix (Fig. 2c). Endolithic hyphae were easily recognised in all samples at a depth of 0.8 mm in the substrate, with coverage ranging from a minimum of 1.7 % in the compact limestone of TSB 38681 to a maximum of 42.1 % in the porous limestone of TSB 37006 (Fig. 3). At a depth of 2.4 mm from the stone surface, hyphae were consistently found in the substrate only in the Roman brick (TSB 44405), with a coverage of 22.7 %, while, in all other samples, penetration was negligible, with less than 1 % coverage (TSB 37006, 37462, 37937, 38683). Some hyphae were still detectable at a depth of 4 mm, but in this case the coverage was negligible, and varied between a minimum of 0.03 % and a maximum of 0.11 % in TSB 35822, 37006, 37937 and 38683 (Fig. 3). These hyphae were always in direct contact with the carbonate clasts. Individual hyphae did not necessarily follow the contact zone between two neighbouring clasts, but were observed to penetrate perpendicularly into the clasts, forming holes with smooth edges (Fig. 2d–f), suggesting that penetration is achieved by active calcite dissolution.

The (bio-)minerals detected by XRD are given in Table 2 (for an example of the relative spectra see Fig. SI 1). Calcite was the main constituent of the substrate in all samples except TSB 44405 (Roman brick, which was rich in quartz and feldspar). Dolomite was only found in low amount in TSB 37462. Two biominerals, whewellite and weddellite - the stable monohydrate and metastable dihydrate forms of calcium oxalate, respectively - were detected in all samples except TSB 37006 (no whewellite) and TSB 44405 (neither form detected with XRD). The minerals analysed by FTIR and their relative abundance are listed in Table 1. High-resolution chemical maps (Figs. 4–6) made it possible to visualise the exact spatial distribution of the compounds in the cross sections. Calcium oxalate, peak at 1315 cm^{-1} (Frost, 2004),

Table 1
Thallus thickness and distribution of calcium oxalate (Ox) and calcite (Cal) according to the FTIR analyses carried out on resin-embedded cross-sections of the specimens of *Tephromela atra* var. *calcarea* from SI Table S1. * both calcite and quartz [Qz] in TSB 33382; **quartz and feldspars in TSB 44405.

TSB	Thallus thickness (mm)	Cortex		Photobiont layer		Medulla		Thallus/substratum interface		Substratum	
		Ox	Cal [Qz]*,**	Ox	Cal [Qz]*,**	Ox	Cal [Qz]*,**	Ox	Cal [Qz]*,**	Ox	Cal [Qz]*,**
33382	1.48	–	n/a	–	-[-]	–	-[+(>)]	–	++ [++(>)]	–	++ [++/+++]
35822	1.01	n/a	n/a	n/a	n/a	–	–	–	++(>)	–	+++
37006	1.22	n/a	n/a	n/a	n/a	++(<)	–	+	++	+	++
37462	0.40	–	–	–	–	–	–	–	++(>)	–	++(>)
37937	0.99	n/a	n/a	n/a	n/a	n/a	n/a	n/a	n/a	n/a	n/a
37940	1.43	+++	n/a	++(<)	n/a	+++	++	++(<)	+++(>)	n/a	++++
37941	0.97	n/a	–	n/a	–	n/a	–	n/a	++(>)	n/a	+++
38681	1.65	++	–	++	–	+(>)	+	++	++(>)	–	+++(>)
38683	0.86	n/a	n/a	n/a	n/a	n/a	n/a	n/a	n/a	n/a	n/a
44405	0.41	+	[-]	++	[-]	++	[+]	+(<)	[++]	–	[++]

-, absent; +, low; ++, medium; +++, high; ++++, very high; <, decreasing with depth; >, increasing with depth; n/a, not analysed.

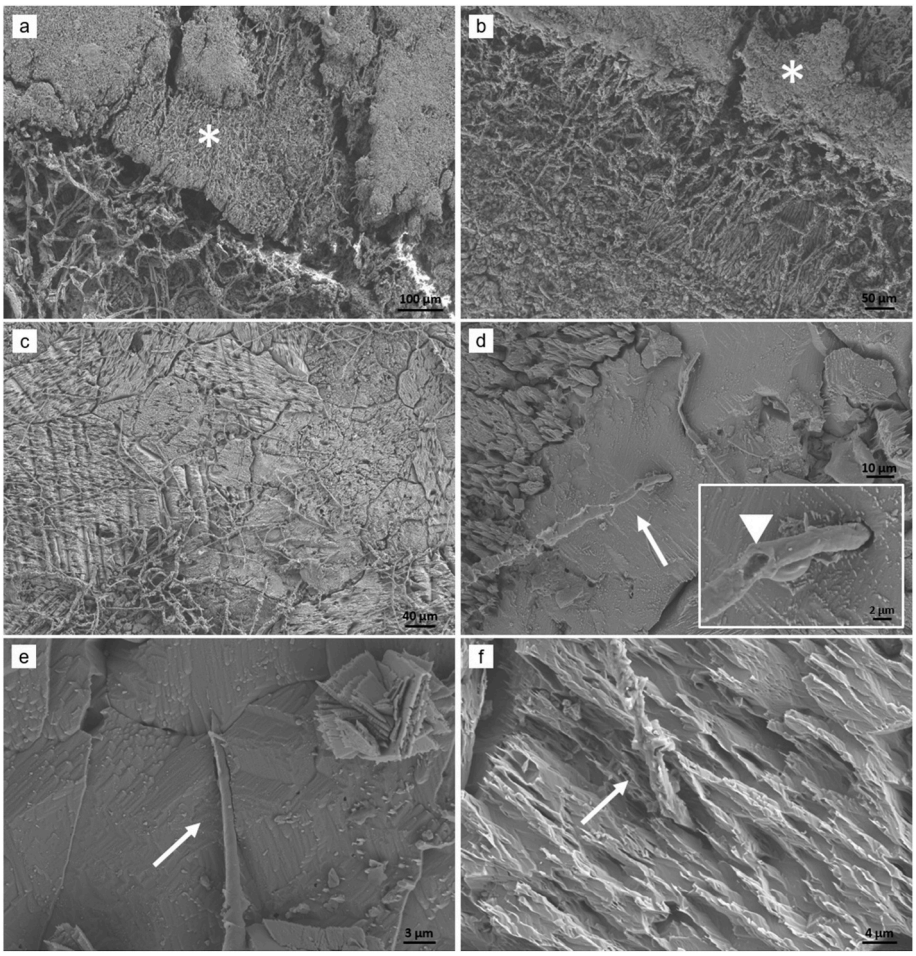

Fig. 2. SEM micrographs of cross-sections of *Tephromela atra* var. *calcarea* stained with periodic acid-Schiff (PAS) showing (a,b) the transition zone between medulla (asterisks) and substrate, which has been partially removed by the acidic PAS stain, revealing the hyphae that were originally within the substrate (calcarenite-calcidurite, TSB 35822, a; bioclastic limestone, TSB 37006, b); (c) network of endolithic hyphae emerging from the partially removed carbonates (bioclastic limestone, TSB 37462); (d–f) individual hyphae (arrows) penetrating calcarenite clasts (TSB 38681, d,e; TSB 35822, f); the insert in Fig. d shows an enlargement of the partially broken hypha (arrowhead) penetrating the substrate.

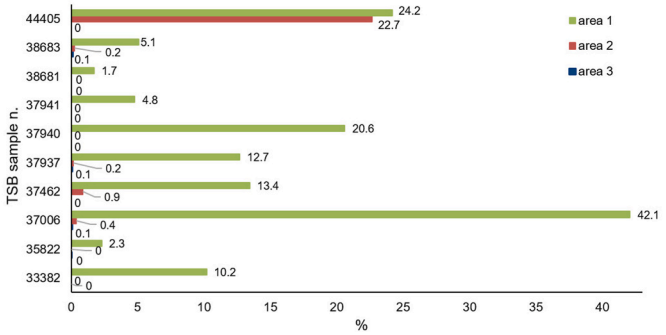

Fig. 3. Hyphal coverage area (%) of the specimens of *Tephomela atra* var. *calcarea* of Table 1 measured in three areas of 2.5 × 0.8 mm each, selected at increasing depths in the substrate as shown in Fig. 1. Further explanations in the main text.

showed a distribution extending from the upper cortex to the thallus–substrate interface (TSB 37940, 38681, 44405 – Fig. 5) or from the medulla to the upper part of the substrate (TSB 37006, data not reported). In both cases the calcium oxalate abundance generally decreased from the thallus to the interface and substratum layers. In some cases, such as TSB 37941, in addition to a decrease in the medulla, a slight increase in the intensity signal was observed at the interface between thallus and substrate, which disappeared in parallel with the disappearance of the hyphae. The characteristic calcite peak (876 cm^{-1}, see White, 1974) was detected in all samples at the interface between thallus and substrate (with medium to high signal intensity), except in TSB 44405 (Roman brick) (Fig. 5a–c,e). Across the analysed cross-sections, however, regions exhibiting variable FTIR signal intensity were observed, suggesting heterogeneous distribution of calcite. Comparison of the FTIR chemical maps with the stereophotographs of the PAS-stained cross-sections (Figs. 4–6) revealed that the areas with less calcite were occupied by hyphae penetrating the substrate. In areas where no hyphae were present, calcite was detected in equal or slightly higher amounts than at the lichen-substrate interface (i.e. the signal intensity was from medium to very high).

4. Discussion

In a study on the thallus–substrate relationships of three lichens occurring on different substrates, including *T. atra*, Salvadori and Tretiach (2002) were able to demonstrate, on the basis of calcium distribution maps by SEM-EDS, that calcareous substrates do not exhibit calcium depletion at the thallus–substrate interface (Salvadori and Tretiach, 2002, Figs. 15–18). From this, they concluded that the carbonate content does not decrease from the rock's interior to the surface when it is colonised by lichen thalli. However, their results cannot be regarded as definitive proof against the "superficial decalcification"

Table 2
Minerals detected by XRD in the specimens of *Tephromela atra* var. *calcarea* from Table S1.

TSB	Calcite	Dolomite	Feldspars	Quartz	Whewellite	Weddellite
33382	+++	–	–	++	+	+
35822	+++	–	–	–	+	+
37006	++	–	–	–	–	++++
37462	++++	+	–	–	+	++
37937	++++	–	–	–	+	+
37940	++++	–	–	–	+	+
37941	+++	–	–	–	+	+
38681	+++	–	–	–	+	+
38683	++++	–	–	–	+	+
44405	–	–	+	++	–	–

-, absent; +, low; ++, medium; +++, high; ++++, very high.

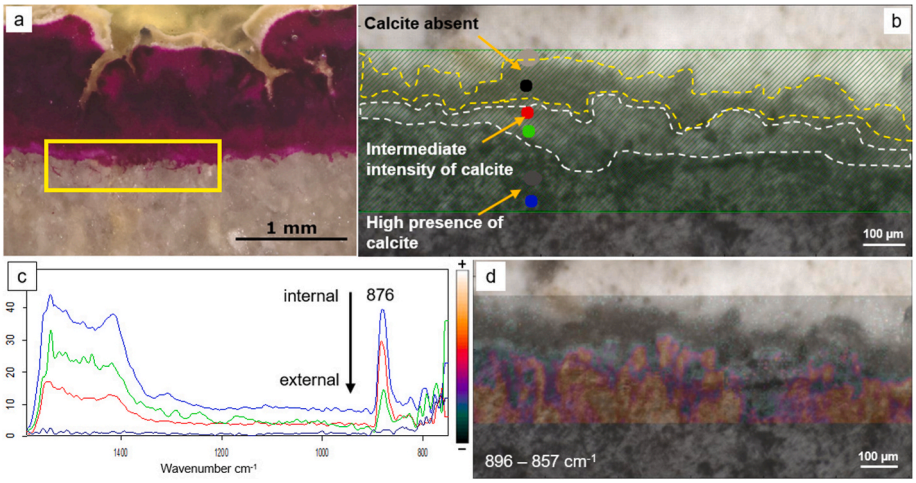

Fig. 4. Cross-section stereophotograph of *Tephomela atra* var. *calcarea* occurring on calcarenite (TSB 37941), stained with periodic acid-Schiff (a); the yellow rectangle corresponds to the area analysed by FTIR, whose results are given in (b) and (c), respectively, showing the morphological map of the analysed area and the extracted spectra of the four selected points, from the inner to the external layers. In (d), calcite distribution map based on the signal recorded at 876 cm^{-1} (c) overlapping the morphological map (a, yellow rectangle). (For interpretation of the references to colour in this figure legend, the reader is referred to the Web version of this article.)

hypothesis, as the mapped calcium ions may be bound not only to carbonate, but also to other anionic groups, in particular oxalates, which are among the most common biomineralization products of some epilithic lichens, and occur also at the thallus–substrate interface (Syers et al., 1967). Perhaps for this reason, other authors have further claimed that "silicicolous" species only occur on calcareous rock when its surface is superficially decalcified (Bültmann, 2012; Bültmann et al., 2015; Nimis et al., 2018; Roux et al., 2025), although they have not provided any experimental evidence for this decalcification. In this work, we identified by XRD (but not unequivocally by FTIR, see below) the two forms of calcium oxalates, the stable monohydrated whewellite (COM) and the metastable dihydrated weddellite (COD) in all specimens of *T. atra* studied, with the exception of TSB 37006 (bioclastic limestone; weddellite only) and TSB 44405 (Roman brick; presence of calcium oxalates suggested by FTIR but not confirmed by XRD). It is worth noting that the lack of clear distinction between the two oxalate forms in FTIR spectra is not due to a limitation of the technique itself – which is, in principle, capable of resolving such differences based on subtle shifts in diagnostic absorption bands (Bazin et al., 2016; Conti et al., 2011; Tonannavar et al., 2016) – but rather to spectral distortions introduced by the reflectance mode, which affected the reliability of band assignments. These XRD-based results confirm the observations of Salvadori and Tretiach (2002), who found that in thalli occurring on siliceous substrates only whewellite is formed, while in calcareous substrates both forms are present, probably due to the high content of calcium ions originating from the progressive dissolution of the carbonate matrix (Giordani et al., 2003). Interestingly, the highest concentration of calcium oxalate crystals occurred in the medulla (Table 1), and in some cases traces of calcium oxalate were also observed inside the rock (*e.g.* in TSB 37006 on bioclastic limestone, see Table 1). The accumulation of calcium oxalate, which in some cases can be quite impressive, explains why the thalli of *T. atra* that occur on calcareous rocks are typically thicker than those on siliceous rocks. For this reason, they were often assigned to a different taxon, which was segregated from the silicicolous taxon [*T. atra* (Huds.) Hafellner var. atra] at the form (*T. atra* f. *pachythallina* Th. Fr.), variety [*T. atra* var. *calcarea* Jatta], or species level [*T. cypria* (Körb.) Hafellner] (Nimis, 2025). However, a taxonomic study by Muggia et al. (2008) based on specimens occurring sympatrically in the Mt. Amiata area (C Italy) on siliceous vs. carbonate-rich rocks has shown that the calcicolous taxon does not form a monophyletic lineage distinct from the silicicolous taxon. This result was confirmed at a global level by a phylogenetic multi-locus analysis (mycobiont nuclear ITS and two protein-coding genes, beta tubulin and the DNA replication licensing factor minichromosome maintenance complex 7), which showed that thalli collected on calcareous rocks are not distinct from specimens collected on other rock types (Muggia et al., 2014).

Even if the calcium map of Salvadori and Tretiach (2002) cannot *per se* refute the hypothesis of "superficial decalcification"due to the diffuse presence of calcium oxalates at the thallus–substrate interface and in the medulla, all the data shown here indicate that *T. atra* can indeed grow in direct contact with the carbonate matrix, whereas the original hypothesis assumes that the lichen is not in direct contact with the carbonate matrix but is isolated by a layer of carbonate-free substrate. Indeed, the chemical imaging performed with FPA-FTIR microscope enabled a

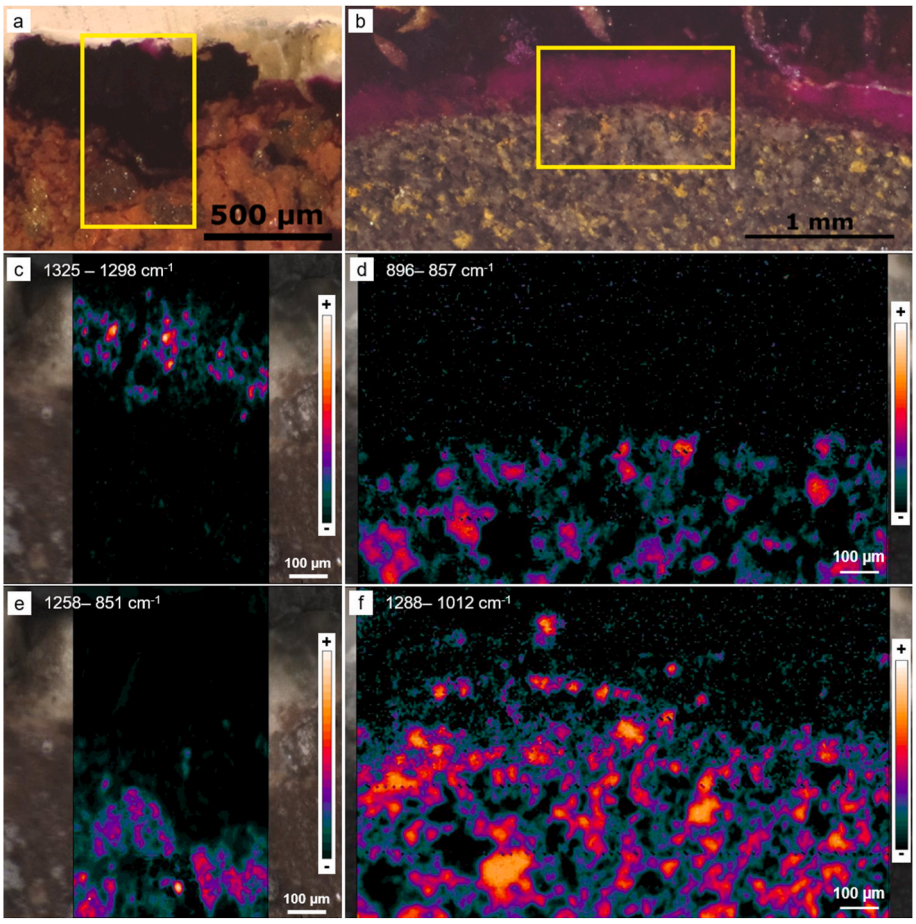

Fig. 5. Cross-section stereophotographs of *Tephomela atra* var. *calcarea* occurring on Roman brick (TSB 44405) (left column: a, c, e) and calcareous schist (TSB 33382a) (right column: b, d, f), stained with periodic acid-Schiff (a, b); the yellow rectangles correspond to the areas analysed by FTIR, with corresponding spatial distribution maps of calcium oxalate (c); calcite (d); quartz and feldspars (e); quartz (f). (For interpretation of the references to colour in this figure legend, the reader is referred to the Web version of this article.)

semi-quantitative description of the calcite profile at the lichen-substrate interface, showing that substantial amounts of calcite are still present under the thalli of *T. atra*, even in the areas heavily colonised by hyphae (Fig. 4b–d). This spatially resolved chemical information was not accessible with earlier approaches. In particular, chemical imaging via FPA-FTIR microscopy represents a significant methodological advance over conventional techniques that lack spatial resolution, as the high sensitivity of this technique enables the deciphering of subtle interactions at microscale bio-mineral interfaces. Our SEM observations are consistent with the FTIR and XRD analyses and show that the hyphae are not only in physical contact with the calcite clasts, especially at the thallus–substrate interface, but can also penetrate them, not through pre-existing cracks or along the contact surfaces between adjacent clasts or crystals, but by forming pits – and probably by an active chemical dissolution not unlike that of euendolithic lichens.

Epilithic lichens can penetrate deep into the substrate with their hyphae, as can be observed when the thallus is removed mechanically, *e.g.* by scraping: Bundles of hyphae remain visible in the interstices of the rock. In siliceous rocks (*e.g.* granite, schist, andesite, etc.), growth usually occurs through the discontinuities of the substrate, as we have seen in the Roman brick (TSB 44405), and along the contact zone of neighbouring rock clasts or crystals, which are thus physically separated by the water-dependent change in the turgor of the hyphae, leading to a progressive weakening of the rock (Ariño and Saiz-Jimenez, 1993). However, the chemical attack on the rock surfaces, which certainly occurs occasionally, as documented by Prieto et al. (1997, 2000), Carballal et al. (2001), Silva et al. (1999) in mica and quartz crystals, is certainly less impressive than the dissolution carried out by euendolithic lichens, i.e. lichens that live almost entirely embedded in the carbonate-rich rock and cause distinct microkarstic corrosion phenomena, from the mesopits produced by their fruiting bodies to furrows along the boundary of two neighbouring thalli (Gehrmann et al., 1992; Pinna et al., 1998; Tretiach, 1995). The hyphae of euendolithic lichens are able to penetrate the individual calcite crystals, in which they form circular holes with a smooth surface (Pinna et al., 1998), clear evidence that this is achieved by chemical dissolution of the carbonates, leading to an increase in substrate porosity (Morando et al., 2017). Here we were able to document (Fig. 2d–f) that *T. atra* is capable of actively chemical dissolving the calcareous matrix, with hyphae that can penetrate perpendicularly into the individual calcite clasts. It must be emphasised that the mechanism of carbonate dissolution by lichens is still largely unknown, although organic acid and respiratory CO_2 release has been occasionally mentioned (Fry, 1924). Notwithstanding this ability in carbonate penetration, that implies the direct metabolic action of *T. atra*, the physical nature of the substrate significantly influences the extent of hyphal penetration by *T. atra*. The minimal hyphal spread in compact limestone compared to that in the more porous bioclastic limestone (Fig. 3) clearly emphasises the role of substrate properties in colonisation efficiency. Differences in the type and extent of porosity have been recognised as relevant factors for determining the extent of fungal colonisation in sedimentary rocks (Cámara et al., 2008), and this finding has been confirmed also in epi- and endolithic lichens (Favero-Longo et al., 2009; Morando et al., 2017).

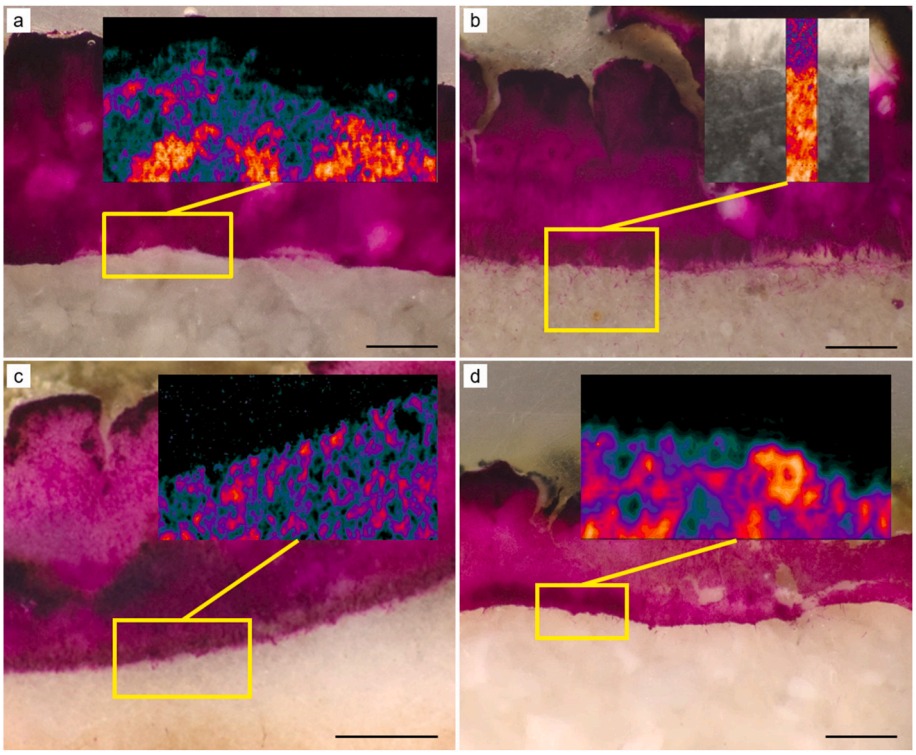

Fig. 6. Calcite distribution maps based on the signal recorded at 876 cm^{-1} by FTIR superimposed on stereophotographs of *Tephomela atra* var. *calcarea*, stained with periodic acid-Schiff, occurring on calcarenites (TSB 38681, a; TSB 37941, b), bioclastic limestones (TSB 37006, c), and calcarenites–calcidurites (TSB 35822, d). Bar = 500 μm.

5. Conclusions

The hypothesis of "superficial decalcification" of carbonate-rich rocks to explain the occurrence of a silicicolous lichen such as *Tephromela atra* was challenged using FTIR distribution maps of calcite and matching stereophotographs of PAS-stained cross-sections. In all samples a high calcite content was found at the interface between the thallus and substrate. Areas with less calcite were occupied by hyphae, some of which were shown to penetrate the calcite clasts, most likely by active chemical dissolution. The occurrence of *T. atra* on carbonate-rich rocks and the intimate contact of its hyphae with the calcite clasts suggest that this lichen has a greater substrate tolerance than expected in terms of pH and mineralogical composition, as it appears to cope successfully with high levels of carbonate, bicarbonate, and calcium ions, which cause the deposition of oxalates (most often whewellite and weddellite, as identified by XRD) in the medulla, with strong morphological changes at the thallus level.

CRediT authorship contribution statement

Mauro Tretiach: Writing – review & editing, Writing – original draft, Visualization, Supervision, Resources, Methodology, Investigation, Funding acquisition, Conceptualization. **Sofia Ceseri:** Writing – review & editing, Writing – original draft, Visualization, Methodology, Investigation, Data curation. **Ornella Salvadori:** Methodology, Investigation. **Francesco Princivalle:** Writing – review & editing, Resources, Methodology, Investigation. **Barbara Salvadori:** Writing – review & editing, Validation, Resources, Methodology, Investigation, Data curation.

Funding

This work was part of the doctoral thesis of S.C., financed by the European Union, Mission 4, component 1, CUP J92B23001630007; part of the costs was covered by D.T.N. (f.o.o.p.) funds from M.T. The acquisition of the Empyrean Malvern Panalytical X-ray diffractometer was made possible by the DE-CARB-FVG project (LR 2/2011, Art. 4, c. 2, letter D, three-year period 2022–2024).

Declaration of competing interest

The authors declare that they have no known competing financial interests or personal relationships that could have appeared to influence the work reported in this paper. .

Appendix A. Supplementary data

Supplementary data to this article can be found online at https://doi.org/10.1016/j.ibiod.2025.106215.

Data availability

Data will be made available on request.

References

Adamo, P., Violante, P., 2000. Weathering of rocks and neogenesis of minerals associated with lichen activity. Appl. Clay Sci. 16, 229–256.

Ametrano, C.G., Selbmann, L., Muggia, L., 2017. A standardized approach for co-culturing Dothidealean rock-inhabiting fungi and lichen photobionts *in vitro*. Symbiosis 73, 35–44.

Appolonia, L., Giamello, M., Sabatini, G., 1996. Caratterizzazione stratigrafica delle pellicole ad ossalati mediante osservazioni in sezione ultrasottile e microdiffrattometria. In: Realini, M., Toniolo, L. (Eds.), *The Oxalate Films in the Conservation of Works of Art. Proceedings 2nd International Symposium*, pp. 359–376.

Ariño, X., Saiz-Jimenez, C., 1993. Granite weathering by the lichen *Rhizocarpon geographicum*. In: Bell, E., Cooper, T.P. (Eds.), Granite Weathering and Conservation, The Director of Buildings' Office. Trinity College, Dublin, pp. 33–35.

Ascaso, C., Galvan, J., 1976. Studies on the pedogenetic action of lichen acids. Pedobiologia 16, 321–331. https://doi.org/10.1016/S0031-4056(23)02187-X.

Ascaso, C., Galvan, J., Rodriguez-Pascual, C., 1982. The weathering of calcareous rocks by lichens. Pedobiologia 24, 219–229. https://doi.org/10.1016/S0031-4056(23)05884-5.

Asta, J., Lachet, B., 1978. Analyses des relations entre la teneur en carbonate de calcium des substrats et divers groupements phytosociologiques de lichens saxicoles. Ecolo. Plant. 13, 193–206.

Asta, J., Roux, C., 1977. Étude écologique et phytosociologique de la végétation lichénique des roches plus ou moins décalcifiées en surface aux étages subalpin et alpin des Alpes françaises. Bull. Mus. Hist. Nat. Marseille 37, 23–81.

Bazin, D., Leroy, C., Tielens, F., Bonhomme, C., Bonhomme-Coury, L., Damay, F., Le Denmat, D., Sadoine, J., Rode, J., Frochot, V., Letavernier, E., Haymann, J.-P., Daudon, M., 2016. Hyperoxaluria is related to whewellite and hypercalciuria to weddellite: what happens when crystalline conversion occurs? C. R. Chim. 19, 1492–1503. https://doi.org/10.1016/j.crci.2015.12.011.

Bültmann, H., 2012. The lichen syntaxa in the checklist of higher syntaxa of Europe – an overview and what we can do with them. Ann. Bot. (Rome) 2, 11–18. https://doi.org/10.4462/annbotrm-9287.

Bültmann, H., Roux, C., Egea, J.M., Julve, P., Bricaud, O., Giaccone, G., Täuscher, L., Creveld, M., Di Martino, V., Golubić, S., Takeuchi, N., 2015. Validations and descriptions of European syntaxa of vegetation dominated by lichens, bryophytes and algae. Lazaroa 36, 107–129. https://doi.org/10.5209/rev_LAZA.2015.v36.51255.

Cámara, B., De los Ríos, A., García del Cura, M.A., Galván, V., Ascaso, C., 2008. Dolostone bioreceptivity to fungal colonization. Mater. Construcción 58, 113–124.

Carballal, R., Paz-Bermúdez, G., Sánchez-Biezma, M.J., Prieto, B., 2001. Lichen colonization of coastal churches in Galicia: biodeterioration implications. Int. Biodeterior. Biodegrad. 47, 157–163.

Conti, C., Colombo, C., Dellasega, D., Matteini, M., Realini, M., Zerbi, G., 2011. Ammonium oxalate treatment: evaluation by μ-Raman mapping of the penetration depth in different plasters. J. Cult. Herit. 12, 372–379. https://doi.org/10.1016/j.culher.2011.03.004.

Edwards, H.G.M., 1997. FT-Raman microscopy of lichen encrustations. Microsc. Anal. 47, 17–19.

Edwards, H.G.M., Perez, F.R., 1999. Lichen biodeterioration of the Convento de la Peregrina, Sahagún, Spain. Biospectroscopy 5, 47–52. https://doi.org/10.1002/(SICI)1520-6343(1999)5:1<47::AID-BSPY6>3.0.CO;2-1.

Edwards, H.G.M., Seaward, M.R.D., 1993. Raman microscopy of lichen-substratum interfaces. J. Hattori Bot. Lab. 74, 303–316.

Edwards, H.G.M., Farwell, D.W., Seaward, M.R.D., 1991. Raman spectra of oxalate in lichen encrustation involved in Renaissance frescoes. Spectrochim. Acta 47A, 1531–1539.

Edwards, H.G.M., Farwell, D.W., Seaward, M.R.D., 1997. FT-Raman spectroscopy of *Dirina massiliensis* f. *sorediata* on diverse substrata. Lichenologist 29, 83–90.

Edwards, H.G.M., Holder, J.M., Wynn-Williams, D.D., 1998. Comparative FT-Raman spectroscopy of *Xanthoria* lichen-substratum systems from temperate and Antarctic habitats. Soil Biol. Biochem. 30, 1947–1953. https://doi.org/10.1016/S0038-0717(98)00065-0.

Edwards, H.G.M., Holder, J.M., Seaward, M.R.D., Robinson, D.A., 2002. Raman spectroscopic study of lichen-assisted weathering of sandstone outcrops in the High Atlas Mountains, Morocco. J. Raman Spectrosc. 33, 449–454. https://doi.org/10.1002/jrs.859.

Edwards, H.G.M., De Oliveira, L.F.C., Seaward, M.R.D., 2005. FT-Raman spectroscopy of the Christmas wreath lichen, *Cryptothecia rubrocincta* Thor. Lichenologist 37, 181–189. https://doi.org/10.1017/S0024282905014611.

Favero-Longo, S.E., Borghi, A., Tretiach, M., Piervittori, R., 2009. *In vitro* receptivity of carbonate rocks to endolithic lichen-forming aposymbionts. Mycol. Res. 113, 1216–1227. https://doi.org/10.1016/j.mycres.2009.08.006.

Fröberg, L., Baur, A., Baur, B., 2006. Field study of the regenerative capacity of three calcicolous lichen species damaged by snail grazing. Lichenologist 38, 491–493.

Frost, R.L., 2004. Raman spectroscopy of natural oxalates. Anal. Chim. Acta 517, 207–214. https://doi.org/10.1016/j.aca.2004.04.036.

Fry, E.J., 1924. A suggested explanation of the mechanical action of lithophilic lichens on rocks (shale). Ann. Bot. 38, 175–196.

Gadd, G.M., 2021. Fungal biomineralization. Curr. Biol. 31, R1557–R1563. https://doi.org/10.1016/j.cub.2021.10.041.

Gehrmann, C.K., Krumbein, W.E., Petersen, K., 1992. Endolithic lichens and the corrosion of carbonate rocks - a study of biopitting. Int. J. Mycol. Lichenol. 5, 37–48.

Giordani, P., Modenesi, P., Tretiach, M., 2003. 'Determinant factors for the formation of the calcium oxalate minerals, weddellite and whewellite, on the surface of foliose lichens'. Lichenologist 35, 255–270.

Gorgoni, C., Lazzarini, L., Salvadori, O., 1992. Minero-geochemical transformation induced by lichens in the biocalcarenite of the Selinuntine monuments. In: Delgado-Rodrigues, J., Henriques, F., Telmo Jeremias, F. (Eds.), Proceedings of the International Congress on Deterioration and Conservation of Stone, LNEC, Lisbon, pp. 531–539.

Holder, J.M., Wynn-Williams, D.D., Rull Perez, F., Edwards, H.G.M., 2000. Raman spectroscopy of pigments and oxalates *in situ* within epilithic lichens: *acarospora* from the Antarctic and Mediterranean. New Phytol. 145, 271–280. https://doi.org/10.1046/j.1469-8137.2000.00573.x.

Mazzotti, V., Rondelli, P., Gualtieri, S., Pinna, D., Magrini, D., 2021. I dolia nel giardino del MIC di Faenza: studio diagnostico per il restauro. Faenza 107, 9–21.

Mitchell, B.D., Birnie, A.C., Syers, J.K., 1966. The thermal analysis of lichens growing on limestone. Analyst 91, 783–789. https://doi.org/10.1039/an9669100783.

Morando, M., Wilhelm, K., Matteucci, E., Martire, L., Piervittori, R., Viles, H.A., Favero-Longo, S.E., 2017. The influence of structural organization of epilithic and endolithic lichens on limestone weathering. Earth Surf. Process. Landf. 42, 1666–1679.

Muggia, L., Grube, M., Tretiach, M., 2008. Genetic diversity and photobiont associations in selected taxa of the *Tephromela atra* group (Lecanorales, lichenised Ascomycota). Mycol. Prog. 7, 147–160. https://doi.org/10.1007/s11557-008-0560-6.

Muggia, L., Pérez-Ortega, P., Fryday, A., Spribille, T., Grube, M., 2014. Global assessment of genetic variation and phenotypic plasticity in the lichen-forming species *Tephromela atra*. Fungal Divers. 64, 233–251. https://doi.org/10.1007/s13225-013-0271-4.

Nimis, P.L., 1993. The Lichens of Italy. an Annotated Catalogue. Museo Regionale di Scienze Naturali, Torino.

Nimis, P.L., 2025. ITALIC - the Information System on Italian Lichens. Version 8.0', University of Trieste, Dept. of Biology. https://dryades.units.it/italic. (Accessed 23 May 2025). released under a CC BY-SA 4.0 licence.

Nimis, P.L., Tretiach, M., 1999. *Itinera Adriatica* - lichens from the eastern part of the Italian peninsula. Stud. Geobotanica 18, 51–106.

Nimis, P.L., Hafellner, J., Roux, C., Clerc, P., Mayrhofer, H., Martellos, S., Bilovitz, P.O., 2018. The lichens of the Alps – an annotated checklist. MicoKeys 31, 1–634. https://doi.org/10.3897/mycokeys.31.23568.

Pinna, D., Salvadori, O., Tretiach, M., 1998. An anatomical investigation of calcicolous endolithic lichens from the Trieste Karst (NE Italy). Plant Biosyst. 132, 183–195. https://doi.org/10.1080/11263504.1998.10654203.

Prieto, B., Silva, B., Rivas, T., Wierzchos, J., Ascaso, C., 1997. Mineralogical transformation and neoformation in granite caused by the lichens *Tephromela atra* and *Ochrolechia parella*. Int. Biodeterior. Biodegrad. 40, 191–199. https://doi.org/10.1016/S0964-8305(97)00052-8.

Prieto, B., Edwards, H.G.M., Seaward, M.R.D., 2000. A Fourier transform-raman spectroscopic study of lichen strategies on granite monuments. Geomicrobiol. J. 17, 55–60.

Rampazzi, L., 2019. 'Calcium oxalate films on works of art: a review'. J. Cult. Herit. 40, 195–214. https://doi.org/10.1016/j.culher.2019.03.002.

Roux, C., et al., 2025. Catalogue des lichens et champignons lichénicoles de France métropolitaine. Revue Et Augmentée, 4e edition. Claude Roux Édit., Mirabeau (Vaucluse), p. 2015.

Salvadori, O., Tretiach, M., 2002. Thallus-substratum relationships of silicicolous lichens occurring on carbonatic rocks of the Mediterranean region. In: Llimona, X., Lumbsch, H.T., Ott, S., Cramer, J. (Eds.), Progress and Problems in Lichenology at the Turn of the Millennium – IAL 4, vol. 82. Bibliotheca Lichenologica, Stuttgart, pp. 57–64.

Salvadori, O., Zitelli, A., 1981. Monohydrate and dihydrate calcium oxalate in living lichen incrustations biodeteriorating marble columns of the Basilica of Santa Maria Assunta on the island of Torcello (Venice). In: Rossi Manaresi, R. (Ed.), Proceedings of the International Symposium the Conservation of Stone II. Centro Conservazione Sculture all'Aperto, Bologna, pp. 379–390.

Scarciglia, F., Saporito, N., La Russa, M.F., Le Pera, E., Macchione, M., Puntillo, D., Crisci, G.M., Pezzino, A., 2012. Role of lichens in weathering of granodiorite in the Sila uplands (Calabria, southern Italy). Sediment. Geol. 280, 119–134. https://doi.org/10.1016/j.sedgeo.2012.05.018.

Seaward, M.R.D., Edwards, H.G.M., Farwell, D.W., 1995. FT-Raman microscopic studies of *Haematomma ochroleucum* (Necker) Laundon var. *porphyrium* (Pers.) Laundon. In: Knoph, J.-G., Schrüfer, K., Sipman, H.J.M., Cramer, J. (Eds.), Contribution to Festschrift Für Dr. Ch. Leuckert, Chemotaxonomy and Geography of Lichens, vol. 57, pp. 395–407. Stuttgart, Bibliotheca Lichenologica.

Seaward, M.R.D., Edwards, H.G.M., Farwell, D.W., 1998. Fourier- transform Raman spectroscopy of the apothecia of *Chroodiscus megalophthalamus* (Müll. Arg.) Vězda and Kantvilas. Nova Hedwigia 66, 463–472.

Silva, B., Rivas, T., Prieto, B., 1999. Effects of lichens on the geochemical weathering of granitic rocks. Chemosphere 39, 379–388.

Syers, J.K., Birnie, A.C., Mitchell, B.D., 1967. The calcium oxalate content of some lichens growing on limestone. Lichenologist 3, 409–414.

Tonannavar, J., et al., 2016. Identification of mineral compositions in some renal calculi by FT Raman and IR spectral analysis. Spectrochim. Acta Mol. Biomol. Spectrosc. 154, 20–26. https://doi.org/10.1016/j.saa.2015.10.003.

Tretiach, M., 1995. Ecophysiology of calcicolous endolithic lichens: progress and problems. G. Bot. Ital. 129, 159–184.

White, W.B., 1974. Infrared Spectra of minerals. In: Farmer, V.C. (Ed.), The Infrared Spectra of Minerals. Mineralogical Society Mononograph, London, pp. 227–284.

Whitlatch, R.B., Johnson, R.G., 1974. Methods for staining organic matter in marine sediments. J. Sediment. Petrol. 44, 1310–1312.

Wilson, M.J., Jones, D., McHardy, W.J., 1981. The weathering of serpentinite by *Lecanora atra*. Lichenologist 13, 167–176.

Wirth, V., 1995. Die Flechten Baden-Württembergs, Teil 1 & 2. Eugen Ulmer GmbH & Co., Stuttgart, p. 1006.